Electronic Supplementary Material (ESI) for Journal of Materials Chemistry A.

Decoupling of Li^+ Conductivity and Mechanical Stability in a Thermally Reversible Concentrated Sulfone-based Gel Electrolyte for Lithium Metal Batteries

Xueao Jiang,[a] *Jiayin Chen*,[a] *Junfeng Zeng*,[a] *Weijian Liu*,[a] *Xuansheng Wu*,[a] *Yang Lv*,[a] *Fangyan Liu*,[b] *Ce Zhang*,[c] *Zhiyong Li*[d], *Xiwen Wang*,*[a] and *Shiguo Zhang**[a]

[a] State Key Laboratory of Advanced Design and Manufacturing Technology for Vehicle, College of Materials Science and Engineering, Hunan University, Changsha 410082, P. R. China. Email: wangxw@hnu.edu.cn; (X. Wang) zhangsg@hnu.edu.cn; (S. Zhang)

[b] Department of Physics, City University of Hong Kong, Hong Kong 999077, Hong Kong.

[c] Nanophotonics and Optoelectronics Research Center, Qian Xuesen Laboratory of Space Technology, China Academy of Space Technology, Beijing 100094, China.

[d] School of Chemistry and Chemical Engineering, Henan Normal University, Xinxiang, Henan 453007, P. R. China.

Experimental section

1. Materials

All materials and operations were stored/performed in an argon-purged glovebox with H_2O and O_2 content < 0.01 ppm. Tetramethylene sulfone (SL) (Aladdin) was dried at 60 °C and stored over molecular sieves. Dimethylformamide (DMF) (Shanghai Titan Scientific Co. Ltd.) was used as received. Methyl cellulose (MC) and 12-hydroxyoctadecanoic acid (12-HOA) were purchased from Sigma-Aldrich and dried at 120 °C. MC had an average molecular weight of 86000 g mol^{-1}, 4,000 cP of viscosity, with methoxy substitution between 27.5-31.5% (weight) and a degree of substitution (D.S., average number of substituent groups attached to the ring hydroxyls) is 1.5-1.9. $LiFePO_4$ (LFP), $Li(Ni_{0.8}Co_{0.1}Mn_{0.1})O_2$ (NCM811) and Bis-(trifluoromethane)sulfonamide lithium salt (LiTFSI) were purchased from Canrd Technology Co. Ltd and dried at 100 °C. Carbon black, PVDF binder, and N-methyl-2-pyrrolidone (NMP) were all purchased from Sigma-Aldrich.

2. Electrolyte preparation

2.1 Preparation of SL electrolyte

In an Ar-filled glove box, 1 mol LiTFSI was dissolved in 2 mol SL and stirred vigorously at 60 °C for 12 h, labeled as concentrated sulfone electrolyte (CSE).

2.2 Preparation of H-GE

In an Ar-filled glove box, different mass concentrations of 12-HOA and CSE were mixed in a clean vial. The system was maintained at 80 °C for 10 min with constant stirring to achieve a clear solution. After the mixed solution was cooled to room temperature (RT) for 10 min, a stable white CSE-based gel with different mass concentrations of 12-HOA was formed, labeled as H-GE. Note that, for preparation of M/H-GE, the mass concentration of 12-HOA correspond to the total mass of the whole system (i.e., 12-HOA, CSE, and MC). However, for the comparison samples without MC, the mass concentration of 12-HOA only corresponded to 12-HOA and CSE.

2.3 Preparation of M-GE

MC is not soluble in CSE in the temperature range between RT to 120 °C. The gelation of MC with DMF occurred after MC was dissolved in DMF, heated to 110 °C and finally cooled to RT. Both CSE and MC are soluble in DMF, and they were dissolved separately in DMF at RT. The CSE dissolved immediately, but the MC required 3 h to dissolve. After completely but separately dissolving 400 mg of MC and 3600 mg of CSE in two beakers containing 20 mL of DMF, the two solutions were mixed. While stirring overnight at RT, the mixed solution was heated to 120 °C and maintained for 1 h to form a gel after cooling to RT. Once the gel was formed, it could be reheated (120 °C) and cooled to achieve a reversible conversion between gel and sol. Thus, the sol can be cast into Teflon Petri dishes by controlling the temperature. After standing overnight in an oven at 75 °C, the oven was evacuated to vacuum for 72 h to evaporate DMF. Finally, the residual DMF was removed by evaporation at RT for 36 h under an Ar-filled glove box, the M-GE film was formed.

2.4 Preparation of M/H-GE

The preparation method of M/H-GE was consistent with that of M-GE. The minority difference was the addition of 120 mg (i.e., 3 wt%) of 12-HOA, the content of MC was reduced from the original 400 mg (i.e., 10 wt%) to 280 mg (i.e., 7 wt%), whereas the content of CSE remained at 3600 mg (i.e., 90 wt%). The subsequent treatments were consistent with the M-GE.

2.5 Preparation of MC scaffold

400 mg of MC was dissolved in 20 mL of DMF, and the solution was heated to 120 °C and maintained for 1 h to form a gel after cooling to RT. Once the gel was formed, it

could be reheated (120 °C) and cooled to achieve a reversible conversion between gel and sol. Thus, the sol can be cast into Teflon Petri dishes by controlling the temperature. After standing overnight in an oven at 75 °C, the oven was evacuated to vacuum for 72 h to evaporate DMF. Finally, the residual DMF was removed by evaporation at RT for 36 h under an Ar-filled glove box, the MC scaffold film was formed.

2.6 Preparation of M/H scaffold

280 mg of MC and 120 mg of 12-HOA were completely but separately dissolved in two beakers containing 20 mL of DMF, the two solutions were mixed. The mixed solution was heated to 120 °C and maintained for 1 h to form a gel after cooling to RT. Once the gel was formed, it could be reheated (120 °C) and cooled to achieve a reversible conversion between gel and sol. Thus, the sol can be cast into Teflon Petri dishes by controlling the temperature. After standing overnight in an oven at 75 °C, the oven was evacuated to vacuum for 72 h to evaporate DMF. Finally, the residual DMF was removed by evaporation at RT for 36 h under an Ar-filled glove box, the MC scaffold film was formed.

3. Characterization

Differential scanning calorimetry (DSC) data were obtained on a DSC822e Mettler-Toledo at a 10 °C min^{-1} heating/cooling rate under an inert atmosphere of nitrogen, and thermogravimetric analysis (TGA) data were acquired on Hitachi STA7200 Thermal Analysis System at a heating rate of 10 °C min^{-1} under the inert atmosphere of Ar. The infrared thermography tests were performed by a Hikmicro handheld infrared thermal imaging camera (H13PRO) to detect the heat dissipation of the LFP||Li-half cells at different times during natural cooling after standing at 80 °C for 1 h. Attenuated Total Reflectance Infrared (ATR-IR) spectroscopy results were measured on the Thermo Scientific Nicolet iS50 spectrometer equipped with a diamond single-reflection Attenuated Total Reflectance (ATR) accessory. Raman spectra were measured on a Thermo Scientific DXR2. Scanning electron microscopy (SEM) and energy-dispersive X-ray spectroscopy (EDS) were performed by FEI Quanta-200F to investigate the structure and morphology of the obtained materials. X-ray photoelectron spectroscopy (XPS) measurements equipped with a vacuum transfer accessory was tested in Thermal Fisher, K-Alpha^{+}. The Al and Li foils were cleaned with SL solvent (without LiTFSI) before XPS and SEM measurements. Rheology measurements were tested using Anton Paar MCR 92 with the laminator in the diameter of 25 mm, cone angle of 1°, and a gap of 0.051 mm (angular frequency=10 rad s^{-1}, strain=1%). The tensile and compressive

properties were measured using a tensile-compressive tester (HY-0580 tension machine). The dog bone-shaped samples (length: 50 mm, width: 4 mm, gauge length: 30 mm) were used in the tensile tests with a velocity of 200 mm min^{-1}. Cylindrical samples (diameter = 25 mm, height = 6 mm) were used for compressive tests.

4. Thermal-induced self-healing

Gel samples with a diameter of 19 mm and a thickness of ~ 80 μm were cut in half, and then the cut surfaces of the two halves were pressed together and allowed to stand at 70 °C for 1 h. The dog bone-shaped samples were used in the tensile tests before and after thermal-induced self-healing with a velocity of 200 mm min^{-1}. The original sample (thickness: 250 μm, width: 4 mm, gauge length: 30 mm). After the fracture, there was an increase in thickness from 250 μm to 300 μm due to the overlapping of the two fracture points being pressed together, while the other parameters remained unchanged.

5. Thermal imaging of Li||LFP cell

Firstly, the Li||LFP cells with various electrolytes were put in an oven at 80 °C for 1 h to ensure uniform heating of the cells, then removed from the oven and placed on the test bench at room temperature. A Hikmicro handheld infrared thermal imaging camera (H13PRO) was pre-fixed 20 cm away from the test bench, and the emissivity was set to 0.25 because the cell shells were made of stainless steel. The heat dissipation of the two cells was detected at different times during the natural cooling process at room temperature.

6. Electrochemical measurements

Li symmetrical cells were assembled to measure the Li^+ transference numbers (t_{Li^+}) of electrolytes. The value was estimated by a combination of DC polarization and AC impedance measurement. The t_{Li^+} value was calculated using the following equation:

$$t_{Li^+} = \frac{I_s(\Delta V - I_0 R_0)}{I_0(\Delta V - I_s R_s)}$$

In which, ΔV was the applied polarization voltage (10 mV), I_0 was the initial current, I_s was the steady-state current, R_0 and R_s were the charge transfer resistance of the Li symmetrical cell before and after polarization, respectively.

Linear sweep voltammetry (LSV) (scan rate: 0.1 $mV \cdot s^{-1}$) and differential pulse voltammetry (DPV) were all measured by Li||SS cells. The pulse width, sample width, pulse period, and quiet time of DPV were set as 0.01 s, 0.0025 s, 0.5 s, and 2 s, respectively. The Li plating/stripping tests were carried out by Li||Li cell at a constant current density of 0.1 mA cm^{-2}. To test ionic conductivity, electrochemical impedance spectroscopy (EIS) was measured using stainless steel symmetrical cells in the

frequency range of 0.01-10^5 Hz from 30 to 70 °C. The ionic conductivity was calculated according to the following equation:

$$\sigma = \frac{L}{R * S}$$

σ was the ionic conductivity, L was the thickness of electrolytes, R was the resistance obtained by EIS, and S was the usable area of electrolytes. The corresponding activation energies were calculated using Arrhenius equation:

$$\sigma(T) = Aexp\left(-\frac{E_a}{RT}\right)$$

Where A was the pre-exponential factor, E_a was the activation energy, and R was the gas constant, T was the temperature (K).

EIS methods of Li symmetrical cells were also used to measure the diffusion coefficients of Li^+ (D_{Li^+}) inside electrolytes, and the values were calculated by the following equations:

$$D_{Li^+} = \frac{R^2T^2}{2A^2F^4C^2\sigma_\omega^2}$$

Here σ_ω is the slope of $Z' \sim \omega^{-1/2}$ obtained from the EIS curve, A is the area of the Li electrode (i.e., the usable area of electrolytes), C is the Li^+ molar concentration inside the electrolyte, F is the Faraday constant (~ 96485 C mol^{-1}), R was the gas molar constant, and T was the absolute temperature.

7. Computational details

The binding energy was calculated by Gaussian 16 quantum chemistry package using B3LYP functionals and 6-311++g(d,p) basis set. The minimum of the analyzed geometries on the potential energy surface was optimized. The vibrational frequency calculations were conducted to correct the free energy. Grimme's DFT-D3(BJ) empirical dispersion correction was used to describe the long-range van der Waals interactions. The formula for calculating binding energy is shown:

$$Eb = E(AB) - E(A) - E(B)$$

The Eb refers to the binding energy, whereas E(AB) represents the energy of the complex formed by substances A and B. E(A) and E(B) denote the individual energies of substances A and B, respectively.

8. Battery performance test

Commercial LFP or NCM811, CNT, and PVDF were mixed in N-methyl pyrrolidone (NMP) with a mass ratio of 8:1:1. Then the mixture slurry was coated on Al foil and dried at 100 °C overnight under vacuum. The normal mass loading of LFP/NCM811 on the cathode was ≈ 1.2 mg cm^{-2}, and the high mass loading of NCM811 was 8.67 mg

cm^{-2}. Finally, the LFP||Li and NCM811||Li half cells were assembled to measure the cycling performance using the LANHE CT2001A and Neware system with the potential range of 2.4−4.2 V and 3−4.3 V, respectively. All the CR2032 cells were assembled in the Ar glovebox using the traditional stacking method. Notably, the liquid comparison cells used Celgard-2400 as separators.

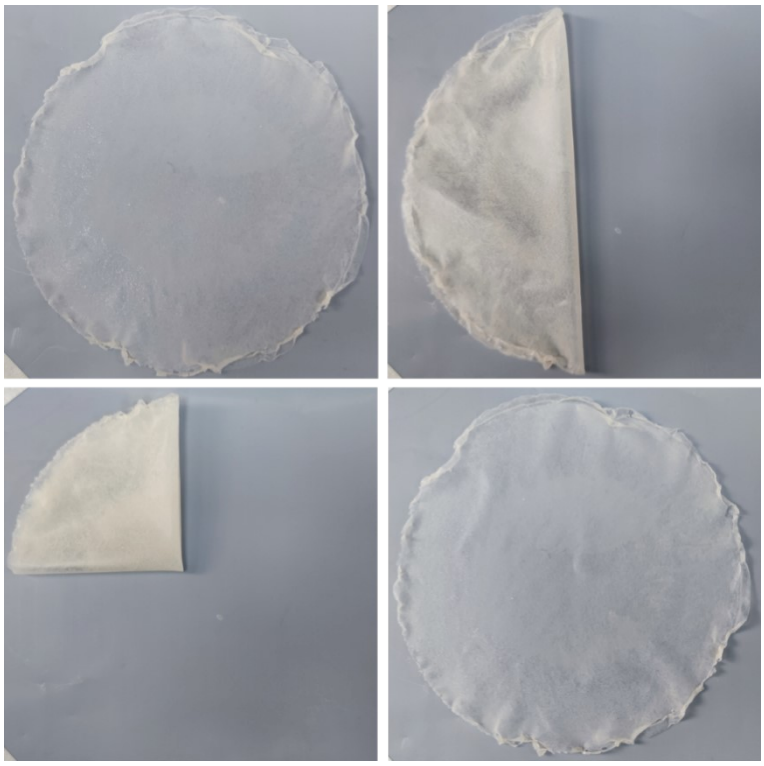

Fig. S1 Digital photographs of M/H-GE membrane.

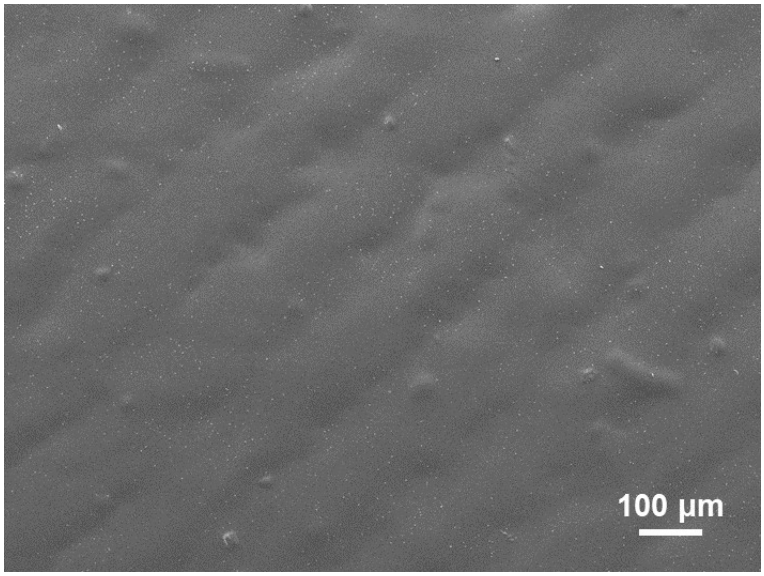

Fig. S2 Top-view SEM image of M-GE membrane using 10 wt% gelator.

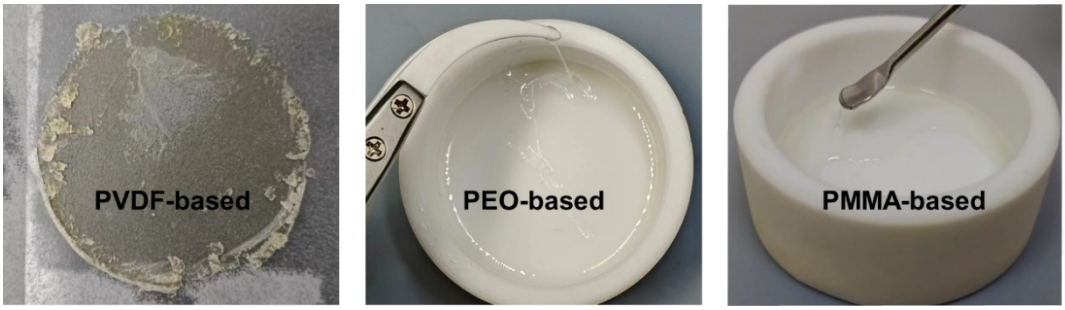

Fig. S3 Digital photographs of 10 wt%PVDF/90 wt%CSE gel, 10 wt% PEO/90 wt%CSE gel, and 10 wt%PMMA/90 wt%CSE gel.

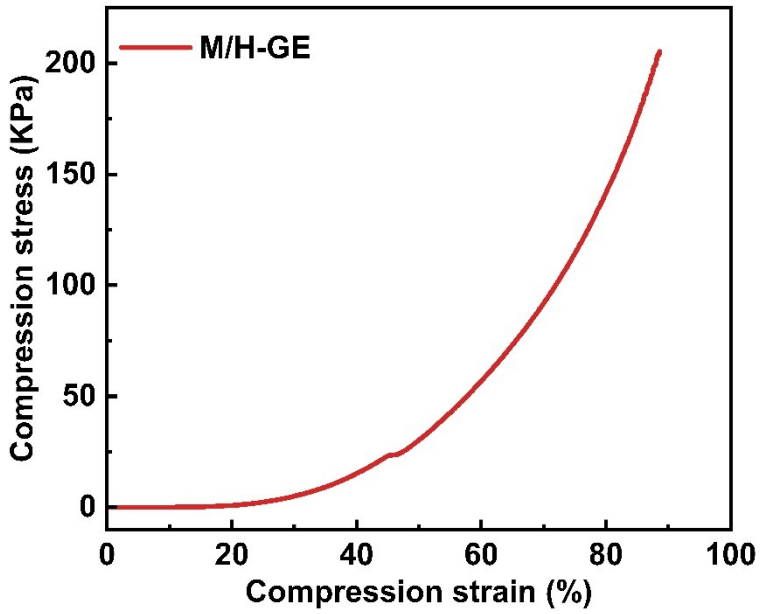

Fig. S4 Compression stress-strain curve of M/H-GE membrane.

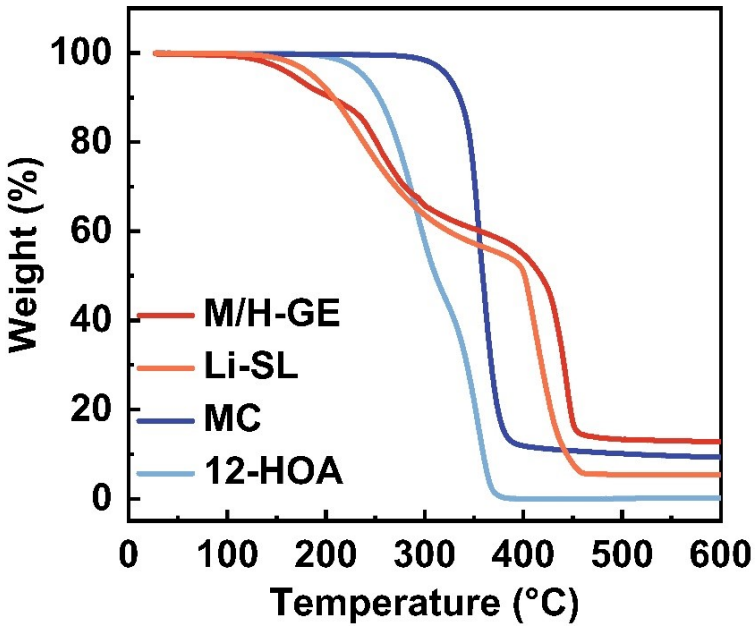

Fig. S5 TGA curves of M/H-GE, MC scaffold, 12-HOA scaffold, and neat CSE electrolyte (Li-SL).

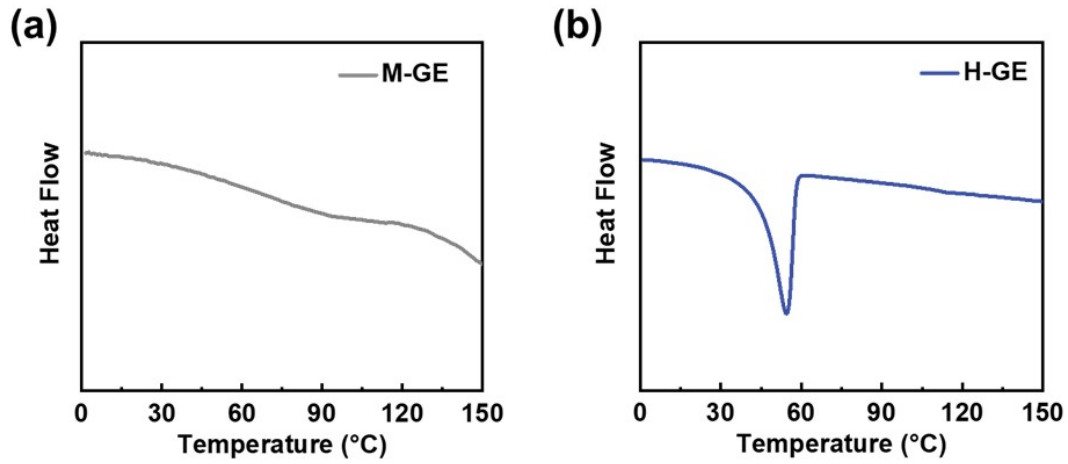

Fig. S6 DSC curves of M-GE, H-GE membrane during the heating process.

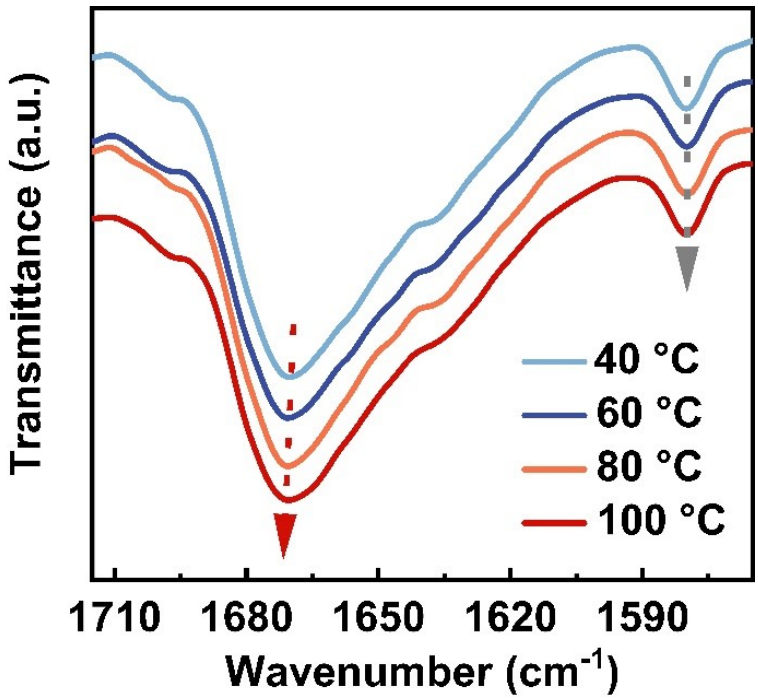

Fig. S7 Temperature-dependent FTIR spectra of M/H-GE membrane in the region of 1565-1725 cm^{-1}.

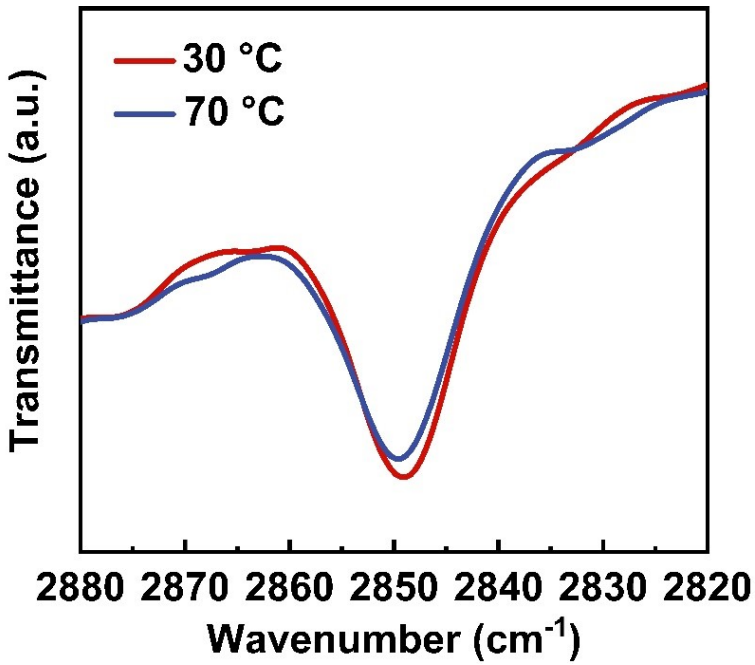

Fig. S8 Temperature-dependent FTIR spectra of M/H-GE membrane in the region of 2820-2880 cm^{-1}.

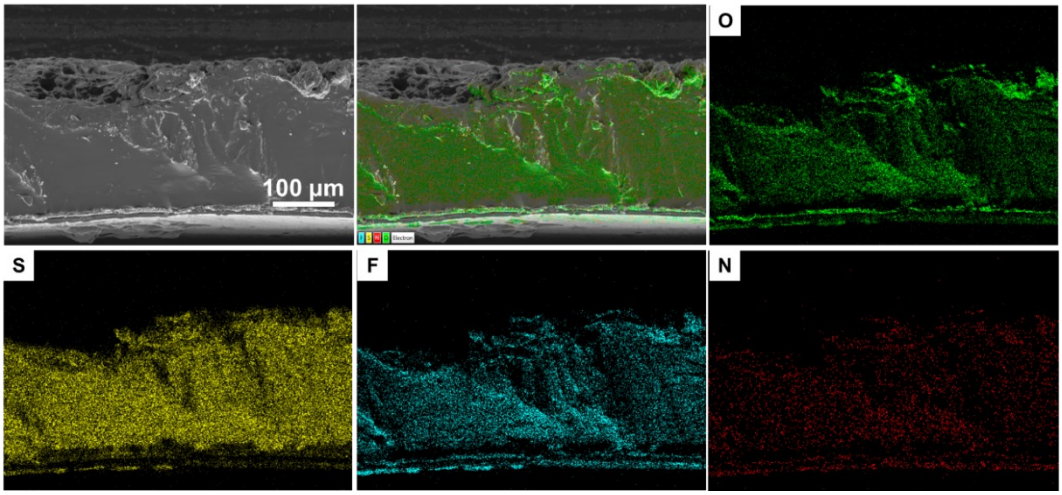

Fig. S9 Cross-sectional SEM images and corresponding EDX mappings of the LFP@M/H-GE integrated electrode.

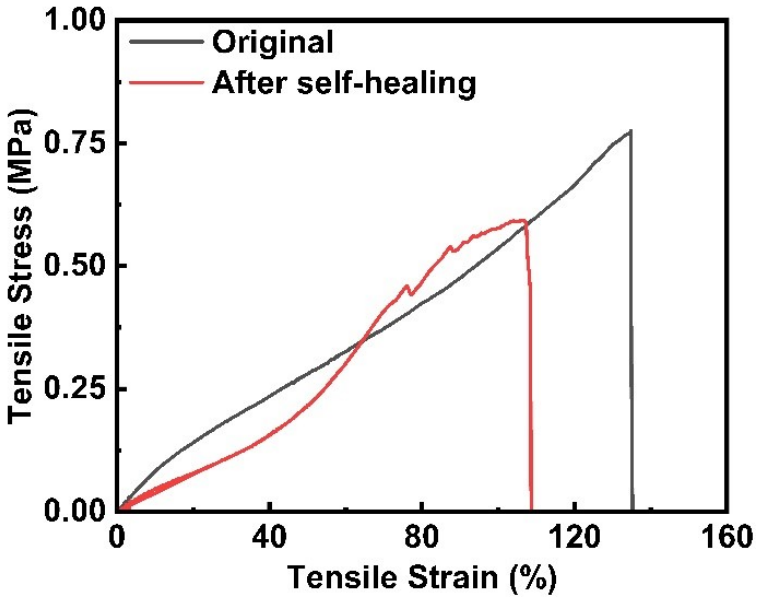

Fig. S10 Tensile stress-strain curves of the cut-healed M/H-GE membranes.

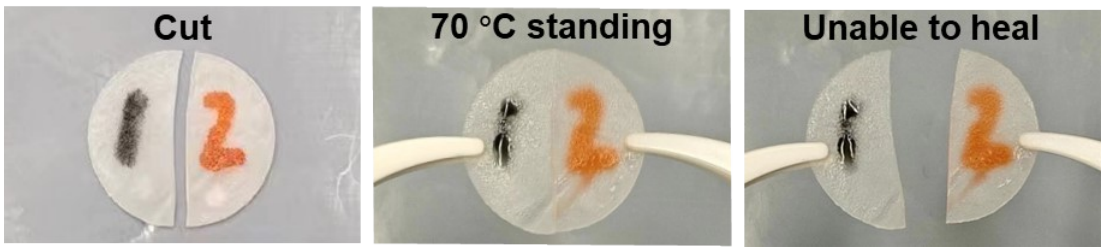

Fig. S11. Photos of the M-GE membranes that were cut into two pieces and then healed at 70 °C.

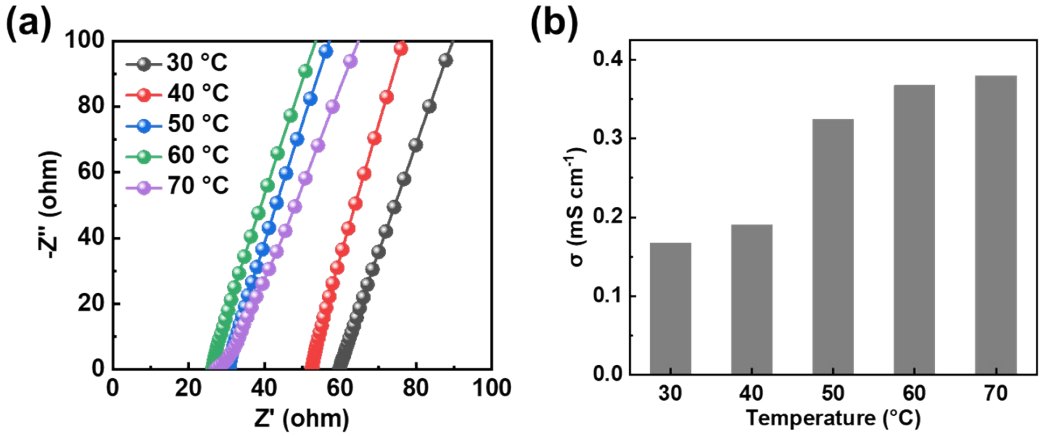

Fig. S12 (a) EIS results and (b) ionic conductivities of stainless steel symmetric cells using the M-GE membrane tested at 30-70 °C.

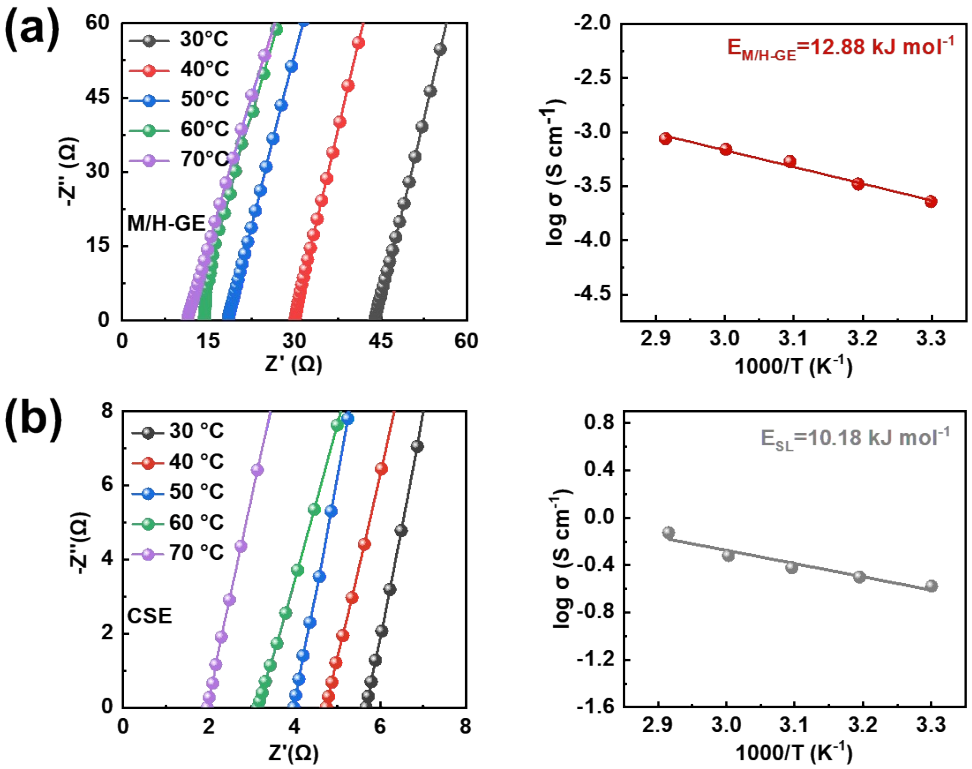

Fig. S13 Temperature-dependent conductivity and Arrhenius plots of M/H-GE and CSE.

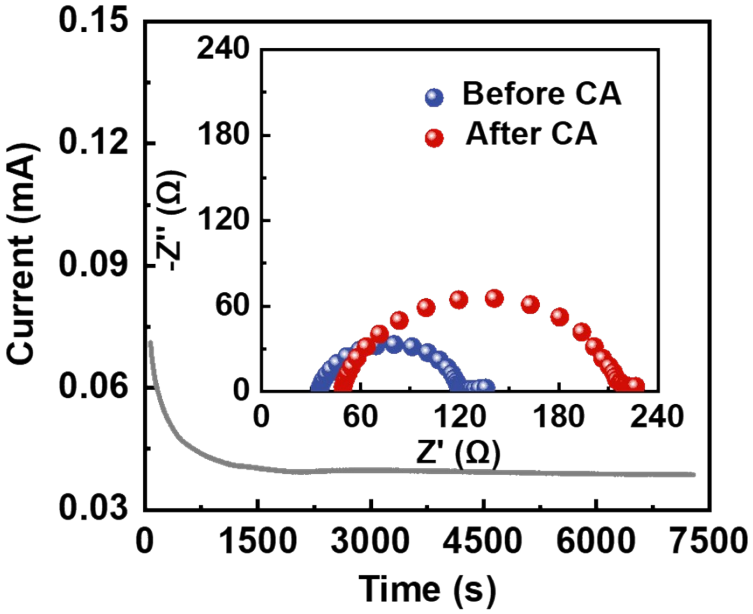

Fig. S14 Direct current (DC) polarization curve of the Li||CSE||Li cell at 10 mV (inset: EIS spectra before and after DC polarization).

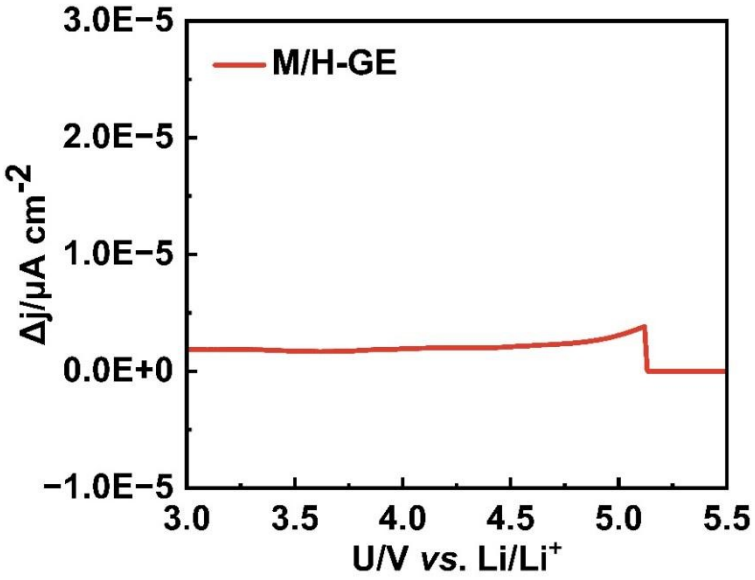

Fig. S15 DPV plot of the Li||M/H-GE||stainless steel cell.

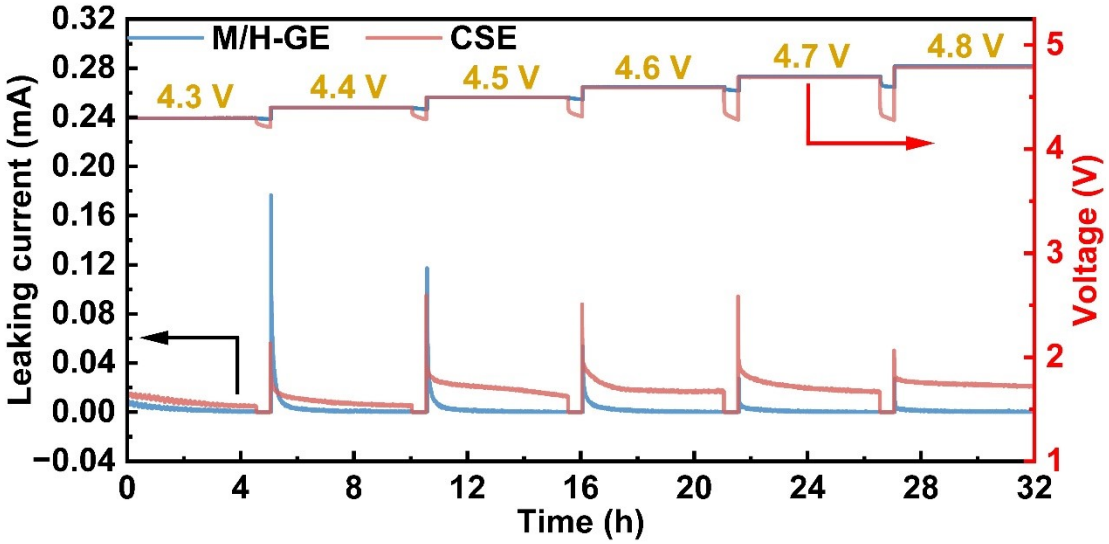

Fig. S16. Floating test of Li||CSE||NCM811 and Li||M/H-GE||NCM811.

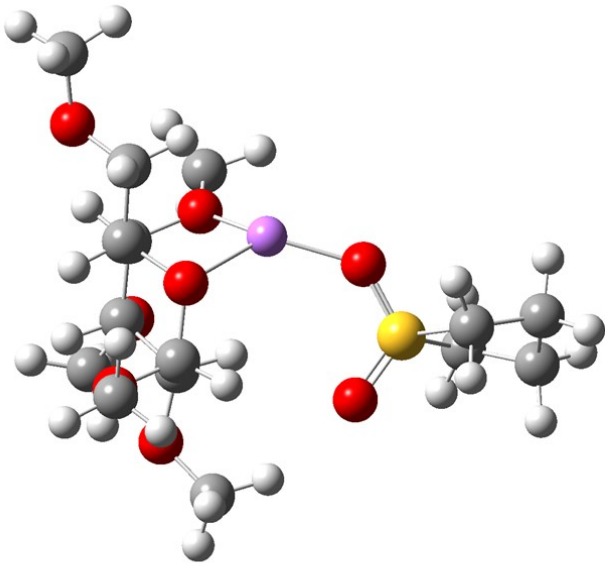

Fig. S17 Simulation of the deformation of $[Li(SL)_2]^+$ complex cation by the interaction between Li^+ and MC.

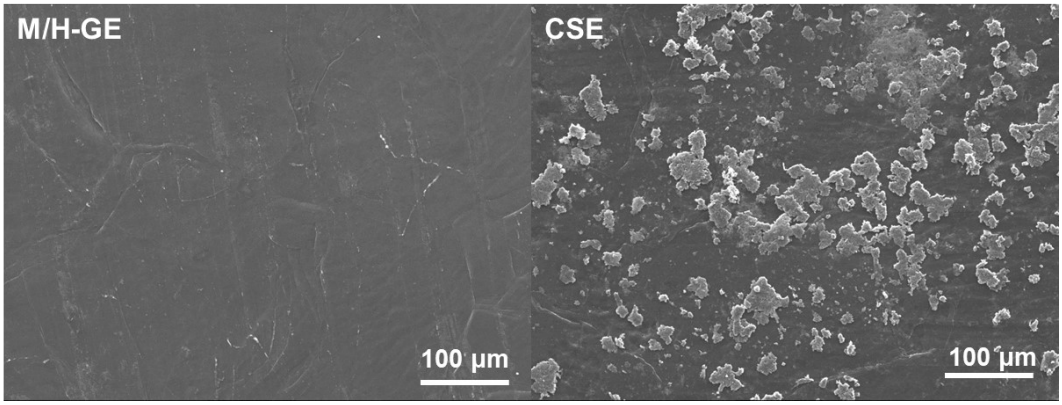

Fig. S18 Low-magnification SEM images deposited lithium surface after 25 cycles using M/H-GE and CSE.

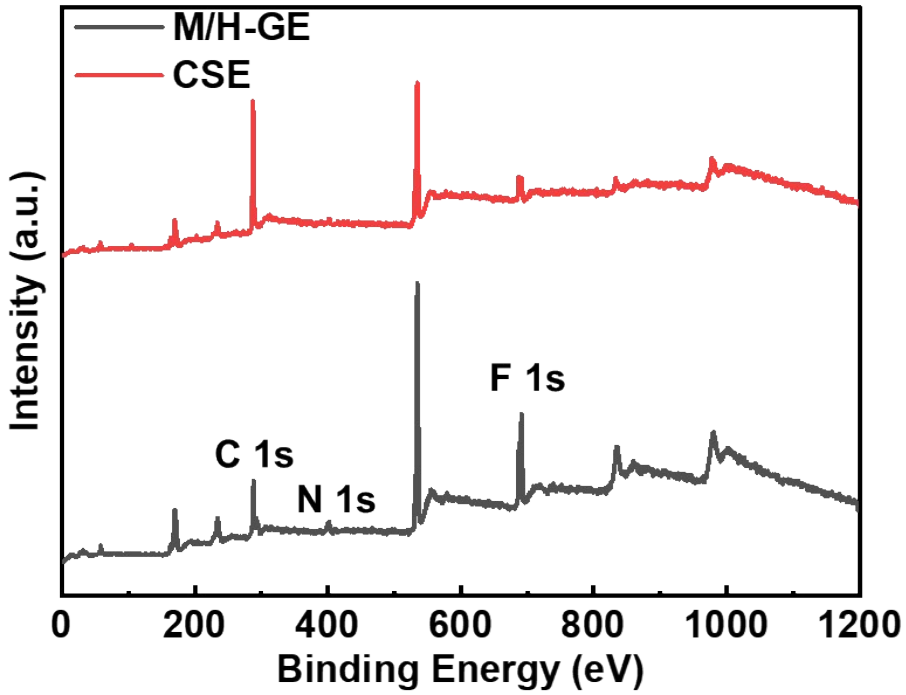

Fig. S19 Full-survey XPS spectra of cycled Li electrode taken from Li||M/H-GE||Li cell and Li||CSE||Li cell.

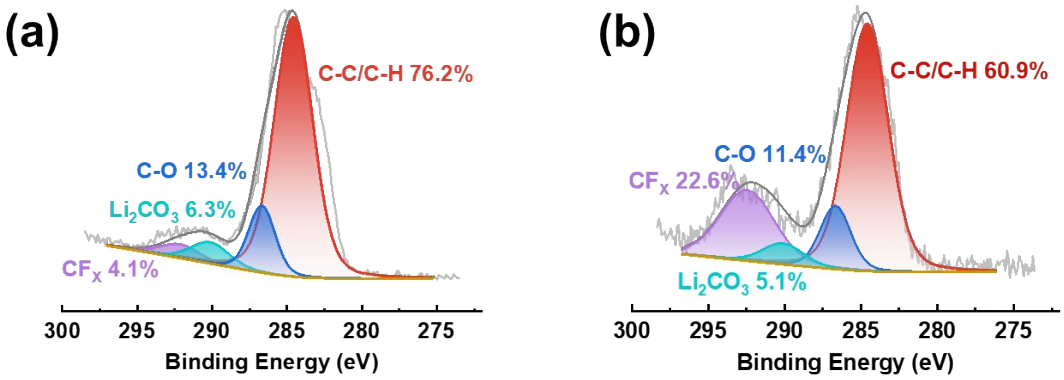

Fig. S20 XPS C 1s spectra of cycled Li electrode taken from (a) Li||M/H-GE||Li cell and (b) Li||CSE||Li cell.

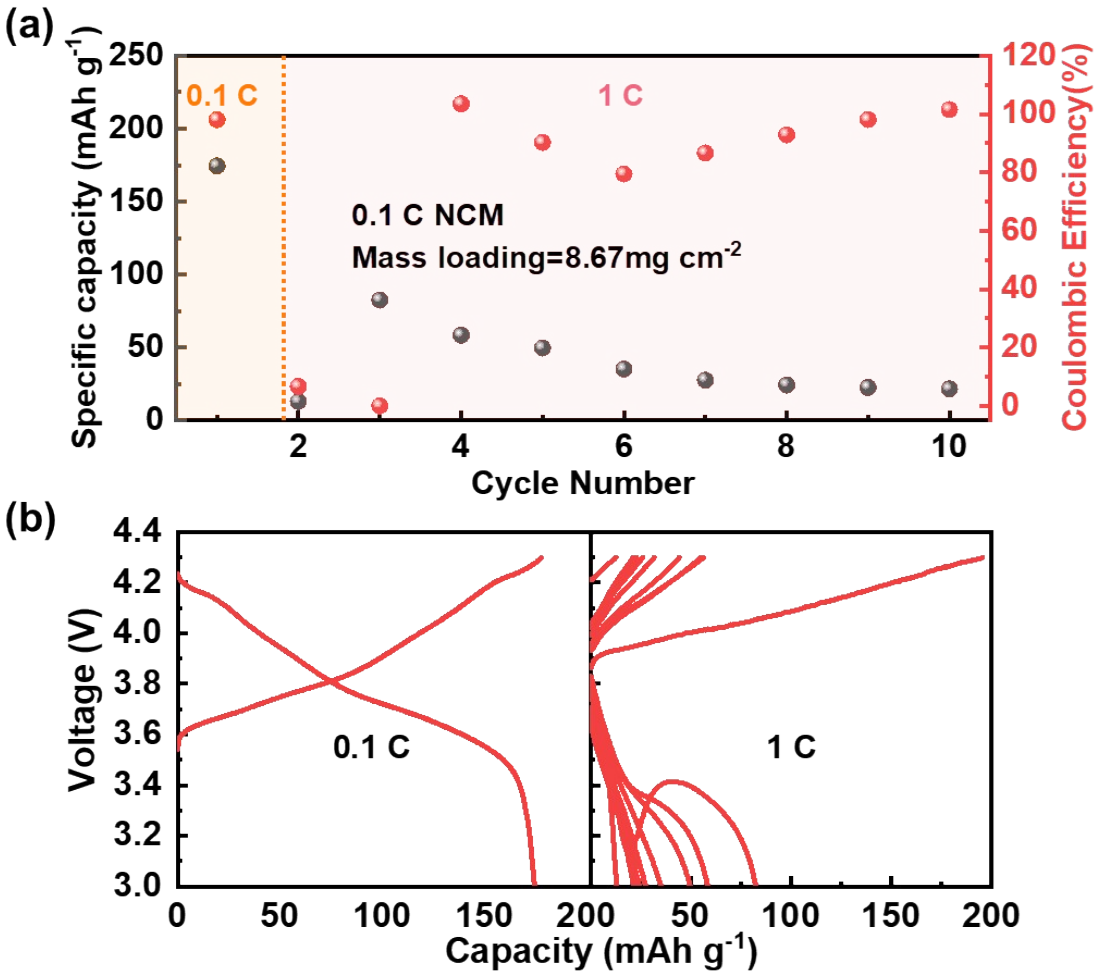

Fig. S21. (a) Cycling performances and (b) charge/discharge profiles of Li||CSE||NCM811 cell at 1 C rate, the first cycle indicated the activation process.

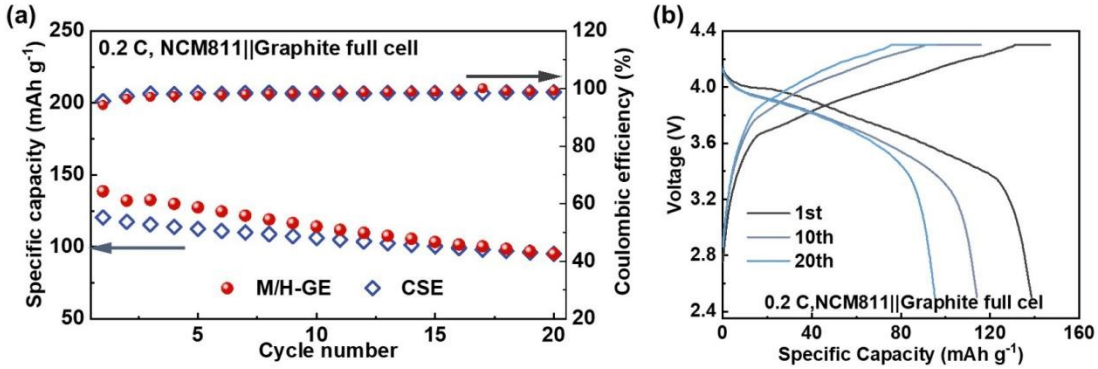

Fig. S22. (a) Cycling performances of Graphite||M/H-GE||NCM811 and Graphite||CSE||NCM811 full cell at 0.2 C, and (b) discharge/charge curves of Graphite||M/H-GE||NCM811 full cell.

Table. S1 Comparison of performance of Li||NCM cell using the ionogels or gels prepared with concentrated electrolytes.

Gel electrolyte	Cathode/Mass loading (mg cm^{-2})	Current Density (C)	Initial/Peak Capacity (mAh g^{-1})	Cycle Number & Capacity decay rate (%)	Ref.
MC/12-HOA@LiTFSI/Sulfone Concentrate electrolyte	NCM811/8.67	1	153.5	400/0.057	**This work**
BN@LiTFSI/Sulfone Concentrate electrolyte	NCM811/1-1.2	0.2	182.4	300/0.054	[9]
12-HOA@[Li(G4)]TFSI solvated ionic liquid	NCM811/1.2	0.1	178.8	200/0.031	[16]
Silica@LiTFSI/[EMIM]TFSI	NCM811/1.2	0.1	182	75/0.010	[58]
LLZO/PMMA@3 M LiTFSI/[EMIM]TFSI	NCM523/1.5	1	139	100/0.1365	[66]
Poly(MPC-co-SBVI)@1 M LiTFSI/[BMP]TFSI	NCM523/12.13	1	90	105/0.1486	[14]
PDMAAm@LiDFOB/Sulfone Concentrate electrolyte	NCM622/10	0.5	167	100/0.090	[65]
PVDF-HFP/Al_2O_3@LiTFSI/[EMIM]TFSI	NCM811/2.0-3.5	0.1	179.1	50/0.3333	[62]
SiO_2@[BMI][TFSI]/LiTFSI	NCM111/	0.1	143.0	100/0.076	[63]
MMA/TEGDMA/ETPTA@LiDFOB/FEC Concentrate electrolyte	NCA/1.7-2.0	0.2	161.4	200/0.0945	[64]